

## DESCRIPTION OF ELECTRICALLY SMALL RESONANT ANTENNAS BY ELECTRIC AND MAGNETIC DIPOLES

D. Pouhè\*, J. A. Tsemo Kamga, and G. Mönich

Technische Universität Berlin, Institut für Hochfrequenz- und Halbleiter-Systemtechnologien, Fachgebiet Antennen & EMV, Einsteinufer 25, D-10587 Berlin, Germany

**Abstract**—A new kind of field representation on the far field sphere is presented. This representation is based upon the polarisation states of the field. Polarisation states can easily be obtained upon determining the peculiar loci in the field. Depending on the polarisation state of the field, it is demonstrated that, either one of the magnetic or the electric dipole moments is dominant. Subsequently, criteria which may be applied to determine which dipole moment is responsible for the main radiation are derived. This characterization scheme which is a good figure of merit for an antenna designer may be useful in mobile communications especially in identifying possible adverse effects of RF fields on human health. The approach is also helpful for EMC engineers seeking to characterize and identify radiation sources of equipment under test.

### 1. INTRODUCTION

The past two decades have seen considerable advances in mobile communication technologies along with the proliferation of end-devices like cell phones, wireless notebooks, etc. to a degree that concerns about adverse effects of electromagnetic (EM) fields on biological tissues have risen in importance. Both the proliferation of electronic devices and the biological effects of EM field place new challenges on the EMC community: The EMC engineer should not only characterize the propagation and absorption of EM energy in tissues, but should also find approaches to avoid or at least to drastically reduce adverse effects on a tissue exposed to an EM field. Furthermore, the EMC

---

*Received 17 May 2011, Accepted 9 July 2011, Scheduled 17 July 2011*

\* Corresponding author: David Pouhè (pouhe@emc.ee.tu-berlin.de).

engineer should quantify and identify radiation sources of equipment under test (EUT) in order to ensure reliability of the product. Sessions held on these issues during major EMC symposia are a vibrant testimony and also reveal their very high rank on the priority list of the EMC community.

The large amount of unknowns and the number of possible combinations in providing quantitative and qualitative comprehensive solutions to these problems make the task very tedious. One of the approach among others is however to take a look at the radiation properties of the device under consideration. The fact that most of the mobile communication devices contain electrically small antennas of arbitrary geometry makes it particularly appealing to go through the radiation of these antennas with a fine-tooth comb. Knowledge of the dipole moment (electric or magnetic) from which the radiation mainly arises can help the antenna designer in making up his mind about the nature of the antenna being designed. For example, purposely designing antennas for cell phones with a predominantly electric behavior is health promoting: it helps limiting the EM energy which can couple into human body, since the maximum and average energy absorptions for a tissue exposed to an EM field arise primarily from magnetic induction [1].

As far as electrically small antennas are concerned, their efficient radiation requires resonances, i.e., the reactive power that in turn implies the existence of both an electric and a magnetic energy storage. These two energy contributions result in corresponding dipole moments. If the magnetic dipole moment is hidden in a stray flux free inductor and only the electric dipole can be observed, then the arrangement is considered to be a small electric dipole or monopole. Alternatively, hiding the electric dipole moment in a capacitor leads to the magnetic dipole. For wire structures, these two options can easily be distinguished. For modern resonant antenna structures of arbitrary geometry however, the task becomes cumbersome. It is almost impossible to distinguish which of the magnetic or the electric behavior is predominantly responsible for the radiation.

This paper aims at generalizing the approach developed in [2] for the decomposition of the radiation of electrically small resonant antennas into the radiation from an electric and a magnetic dipoles. For the sake of completeness “short-cuts” adopted in our discussion in [2] are avoided. Nevertheless, some parts of [2] will be repeated here below not only to ensure a smooth and continuous reading from one section to another but also to provide readers with an interesting discussion about the “*ins and outs*” of the method.

The decomposition of small resonant antennas into electric and

magnetic elementary dipoles is demonstrated by taking canonical structures like bent wire and mini-loop as examples (Section 2). Section 3 is devoted to the decomposition of the field radiated by an antenna of arbitrary geometry. Polarisation plays a role of equal importance in antennas and waves propagation as it can convey significant identification information about the antenna being used, radar targets, etc. [3, 4]. Due attention is therefore given in Section 4 to the concept of far-field polarisation. The phenomenology of the analysis is presented and validated in light of considerations elaborated in Section 3. The aim is to provide a new valuable approach for visualizing the state of polarisation on the far-field sphere. Circular and linear polarisation are here of particular interest. The graphical representation of these different polarisation states is the subject matter of Section 5. Section 6 imparts insights into the dipole moment mainly responsible for the radiation and characterizes dipoles into dominant and non-dominant dipoles.

## 2. ASSIGNMENT OF THE THREE CURRENT DENSITY TO THE DIPOLE MOMENTS

The Maxwell total current density  $\mathbf{J}^t$  can be expressed as the sum of the conduction current  $\mathbf{J}^c$  and the displacement current  $\mathbf{J}^d = \frac{\partial \mathbf{D}}{\partial t}$

$$\mathbf{J}^t = \mathbf{J}^c + \frac{\partial \mathbf{D}}{\partial t} \tag{1}$$

and is divergence free. The three currents, i.e.,  $\mathbf{J}^t$ ,  $\mathbf{J}^c$  and  $\frac{\partial \mathbf{D}}{\partial t}$ , should be distinguished, because

- a)- on metal, at places where lines of the flux density  $\mathbf{D}$  end, electric charges are present;
- b)- time varying surface charges are present at places where lines of current displacement end. These are places where the divergence of the conduction current,  $\nabla \cdot \mathbf{J}^c$ , which is responsible for the electric dipole moment, does exist. Therefore, the surface charges can be determined from  $\nabla \cdot \mathbf{J}^c$  or  $-\partial \mathbf{D} / \partial t$ .

A consequence from the aforementioned nomenclature is that the total current  $\mathbf{J}^t$  can be used for the determination of the magnetic dipole moment, since it is divergence free; while  $\frac{\partial \mathbf{D}}{\partial t}$  will be used to obtain the electric dipole moment. Equation (1) may therefore be rewritten as

$$\mathbf{J}^c = \underbrace{\mathbf{J}^t}_{\text{deter. of magn. dipole moment}} - \underbrace{\frac{\partial \mathbf{D}}{\partial t}}_{\text{deter. of elec. dipole moment}}, \tag{2}$$

whereby  $\partial \mathbf{D} / \partial t$  is only considered by such lines, which still land on the metal, not however from already detached ones (Figs. 1(a) and 2(a)).

Equation (2) suggests that if the magnetic dipole moment is hidden in a stray flux free inductor and only the electric dipole can be observed, the arrangement is then considered to be a small electric dipole or a monopole. Alternately, hiding the electric dipole moment in a capacitor leads to the magnetic dipole. For canonical wire structures like a bent wire or mini-loop, these two options can easily be distinguished.

As an illustration, consider the wire antennas of Figs. 1(a) and 2(a). A triangular current distribution varying along the antennas assumed, the conduction currents produced by the source through the wire may then be decomposed into closed currents circulating clockwise around loops of different sizes (divergence free current) and vertical currents (displacement currents) depositing periodically charges at the bottom and the top of the loop (Figs. 1(b) and 2(b)). The closed currents form a magnetic dipole moment, whereas the charges at the bottom and at the top of the antenna generate an electric dipole.

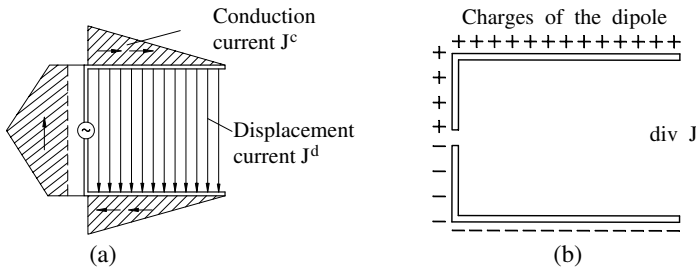


**Figure 1.** Decomposition of a bent wire in electric and magnetic dipole moments. (a) Triangular current along the antenna decomposed into closed currents and displacement currents. (b) Charges deposited by displacement currents.

Equation (2) describes in reality three dimensional currents. Nevertheless, the examples illustrated are precise models although their graphs only show two dimensional currents. Recall that, despite the negative sign, the divergence in either dimension remains the same.

For electrically small resonant antenna structures of arbitrary geometry, the task of distinguishing the two options mentioned here above is more complicated. Common representation only allows the decomposition into electric and magnetic dipole moments with an arbitrary phase between the dipole moments [5,6]. Consequently, the fields have more possibilities. However, the resonant character of the antennas under consideration here necessarily requires electric and

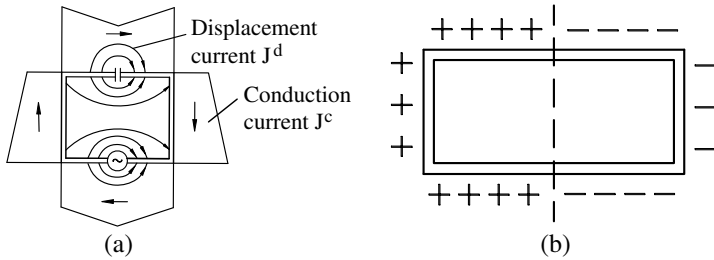


**Figure 2.** Decomposition of a mini-loop in electric and magnetic dipole moments. (a) Triangular current along the antenna decomposed into closed currents and displacement currents. (b) Charges deposited by displacement currents.

magnetic dipole moments to be coercively  $90^\circ$  out of phase. Indeed, this condition is properly met, since the charge maximum and the current maximum are  $90^\circ$  out of phase which in turn makes the well known spherical-wave expansion after Hansen [5] not necessarily applicable in this case. The application of the spherical-wave expansion approach would result in three electric and three magnetic dipoles requiring a huge amount of data on the whole sphere. In addition, it is almost impossible to distinguish which of the magnetic or the electric behavior is predominantly responsible for the radiation. Therefore, a new kind of field representation on the far field sphere is called for. We deal with this point in Section 4. Prior to that, let us decompose the radiated field of an antenna of arbitrary geometry into radiations produced by elementary dipoles.

### 3. DECOMPOSITION OF THE RADIATED FIELD INTO RADIATIONS FROM ELEMENTARY DIPOLES

Let us consider an electrically small antenna as depicted in Fig. 3. The resonant character of the antenna permits considering only contributions from dipoles, since higher order multipoles do not play a major role [7–9]. In fact, for normal-gain radiators the contribution of higher order multipoles to the radiating power is negligibly small, less than 1% [8].<sup>†</sup> Moreover, because of the aforementioned character,

<sup>†</sup> For an arbitrary small antenna, a high directivity can theoretically be obtained. This does not however mean that the contribution of higher order multipoles to the radiated power is significant. As demonstrated by Harrington in [7] and later reproduced by Zinke and Brunswig in [9], upon expanding the field radiated by an arbitrary antenna in spherical coordinates, the contribution of higher-order multipoles to the overall radiated power remains negligible. Field strengths arising from higher expansion terms mainly contribute to the reactive power for normal gain antennas.

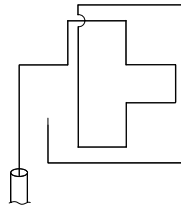


**Figure 3.** Antenna of arbitrary geometry.

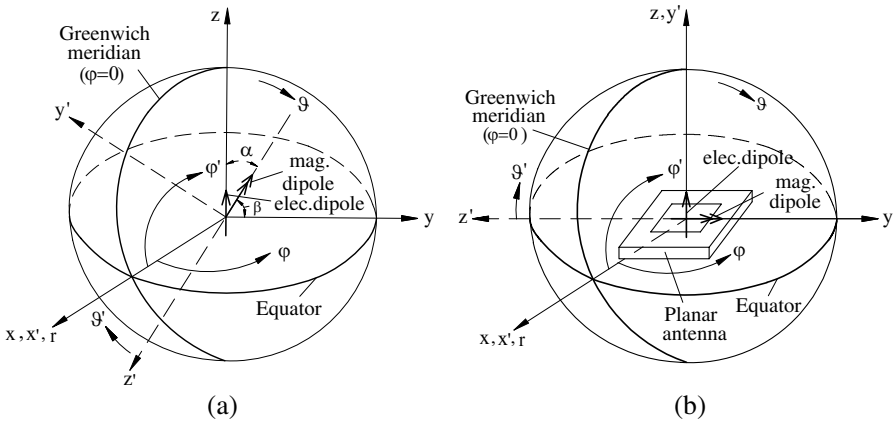


**Figure 4.** (a) Equivalent dipole for calculating the total field of an arbitrary antenna. (b) Planar antenna with equivalent dipoles for calculating the total field in spherical coordinates. The electric dipole is associated with  $r$ ;  $\vartheta$ ;  $\varphi$  while its magnetic counterpart is associated with  $r'$ ;  $\vartheta'$ ;  $\varphi'$ .

all electric dipole moments are coercively in phase. As a result, many electric dipole moments can be summed up into a single one. This also applies for magnetic dipoles. Therefore, the overall field radiated by the antenna can be seen as emanating from a combination of an electrical dipole associated to the cartesian coordinate system  $x, y, z$  and a magnetic dipole associated to the prime coordinates  $x', y', z'$  (Fig. 4):

$$\mathbf{E} = \mathbf{E}^e + \mathbf{E}^m. \tag{3}$$

In the far field region,  $\mathbf{E}^e$  and  $\mathbf{E}^m$  build an electric angle of  $\pi/2$ .

For simplicity, the electric dipole moment is assumed vertically oriented along the  $z$  axis throughout this work whereas the magnetic dipole moment is aligned with the  $z'$  axis. Their respective spherical coordinates are  $r, \vartheta, \phi$  for the electric dipole and  $r', \vartheta', \phi'$  for the magnetic dipole. The two dipoles build an angle  $\alpha$  ( $0 \leq \alpha \leq \pi/2$ )

to each other and their respective coordinates are also related through the following transformation

$$\begin{pmatrix} x' \\ y' \\ z' \end{pmatrix} = \underbrace{\begin{pmatrix} 1 & 0 & 0 \\ 0 & -\cos \alpha & \sin \alpha \\ 0 & -\sin \alpha & -\cos \alpha \end{pmatrix}}_M \cdot \begin{pmatrix} x \\ y \\ z \end{pmatrix} \quad (4)$$

whereby  $M$  is the transformation matrix.

The electric field of the magnetic dipole can be expressed temporarily in the non-prime Cartesian system as (see details in the Appendix)

$$\mathbf{E}^m = -\frac{E_m}{r} [(\cos \alpha \sin \vartheta \sin \phi - \sin \alpha \cos \vartheta) \cdot \mathbf{e}_x - \cos \alpha \sin \vartheta \cos \phi \cdot \mathbf{e}_y + \sin \alpha \sin \vartheta \cos \phi \cdot \mathbf{e}_z], \quad (5)$$

where

$$E_m = -\frac{\omega \mu I_0}{4\pi} A k e^{-jkr}. \quad (6)$$

For convenience, the distance phase term  $e^{-jkr}$  is dropped and throughout the rest of this work,  $E_m$  is taken to be

$$E_m = -\frac{\omega \mu I_0}{4\pi} A k. \quad (7)$$

As we are seeking a new kind of field representation on the far field sphere, (5) may be transformed in spherical coordinates using the well known transformation matrix from Cartesian to spherical coordinates [3]. Performing the necessary algebra we get (see Appendix)

$$E_r^m = 0, \quad (8a)$$

$$E_\vartheta^m = \frac{E_m}{r} \cos \varphi \sin \alpha, \quad (8b)$$

$$E_\phi^m = \frac{E_m}{r} (\sin \vartheta \cos \alpha - \sin \varphi \cos \vartheta \sin \alpha). \quad (8c)$$

For the special case of planar antennas where the two dipoles are orthogonal, i.e.,  $\alpha = \pi/2$ , (8) simplifies and becomes [2]

$$E_r^m = 0, \quad (9a)$$

$$E_\vartheta^m = \frac{E_m}{r} \cos \varphi, \quad (9b)$$

$$E_\phi^m = -\frac{E_m}{r} \sin \varphi \cos \vartheta. \quad (9c)$$

Note that the aforementioned transformation from rectangular to spherical components is a straightforward process.

The electric field component of the electric dipole is in turn given by

$$\mathbf{E}^e = E_{\vartheta}^e \mathbf{e}_{\vartheta} = \frac{E_e}{r} \sin \vartheta \cdot \mathbf{e}_{\vartheta}, \quad (10)$$

with  $E_e$  being

$$E_e = -\frac{I_0 \Delta z}{4j\omega\varepsilon\pi} k^2 e^{-jkr}. \quad (11)$$

Again, as for the case of the magnetic dipole moment, the distance phase term  $e^{-jkr}$  is dropped for convenience and  $E_e$  throughout the rest of this work becomes

$$E_e = j \underbrace{\frac{I_0 \Delta z}{4\omega\varepsilon\pi} k^2}_{E_e^0} = jE_e^0. \quad (12)$$

In the equations above, the superscript/subscript  $e$  and  $m$  indicate the electric and magnetic fields respectively. The total field (Equation (3)) in the far field region can now be expressed as

$$\mathbf{E} = \mathbf{E}_{\vartheta} + \mathbf{E}_{\varphi} = E_{\vartheta} \mathbf{e}_{\vartheta} + E_{\varphi} \mathbf{e}_{\varphi} = (E_{\vartheta}^e + E_{\vartheta}^m) \mathbf{e}_{\vartheta} + E_{\varphi}^m \mathbf{e}_{\varphi}. \quad (13)$$

Note that  $\mathbf{E}_{\vartheta}$  and  $\mathbf{E}_{\varphi}$  have a geometric angle of  $\pi/2$ .

#### 4. FAR FIELD POLARISATION ANALYSIS

So far, it has only been shown mathematically that a radiated field from an antenna can be decomposed into fields emanating from elementary electrical and magnetic dipoles. One of the two dipoles may, however, be mainly responsible for the radiation under certain conditions. It might also be necessary to know the orientation of the dipole moments. For example, if the antenna has characteristics of a loop, the magnetic dipole may be dominant and its orientation easily determined. This is however not the case for the antenna depicted in Fig. 3 or modern resonant antennas commonly used nowadays in mobile phones.

An approach which may help us to gain more insight into the aforementioned issues is the representation of the fields on the far field sphere. This representation, as shown in the following, is based upon the polarisation states of the field.

### 4.1. Phenomenology of the Approach

Polarisation states might easily be obtained upon determining the peculiar loci in the field. These loci can be found along

- a)- the lines of linear polarisation (LLP) — Here  $E_\theta$  and  $E_\varphi$  are in phase,  $\widehat{E_\theta, E_\varphi} = 0$ , or  $180^\circ$  out of phase,  $\widehat{E_\theta, E_\varphi} = \pm\pi$ ,
- b)- the symmetry line which is the line where the electric field components are orthogonal ( $\widehat{E_\theta, E_\varphi} = \pi/2$ ) and
- c)- the lines of equal amplitudes ( $|E_\theta| = |E_\varphi|$ ).

All these lines are schematically graphed in Fig. 5. As can be seen, the LLP must be closed, since they separate the area with left hand polarisation sense from the area with right hand sense. The existence of zeros in the pattern along the axis of each dipole leads to an overall field consisting only of the field from the other dipole for linear polarisation. Both axes of the dipoles must therefore break through the sphere at points located on the LLP, when circumscribed in a sphere of radius  $r$ .

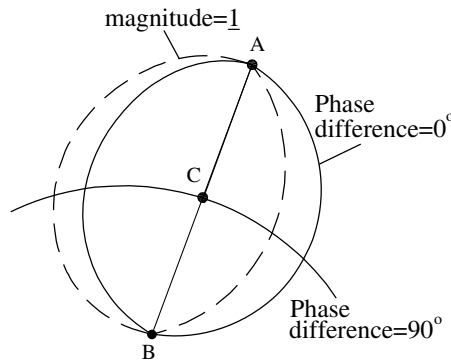


**Figure 5.** Lines on which peculiar loci of the field can be found.

The lines of equal amplitudes may also be closed curves. They may intersect the lines of linear polarisation at least at two points  $A$  and  $B$ . That is, two different phase differences at one point are required. This contradiction can only be resolved if either  $E^e$  or  $E^m$  vanishes in  $A$  and  $B$  thereby making the phase undefined. As a result, the axes of the two dipoles are found in  $A$  and  $B$ . In fact, their axes pass through  $A$  and  $B$  respectively. The lines, where the electric fields are orthogonal, are big circles or half circles for patch structures with ground plane. Their intersection point  $C$  with the curve of equal amplitudes which lies within the area delineated by the line of linear polarisation indicates the point of circular polarisation. Circular polarisation requires however

equal amplitudes as well as geometric and electric orthogonality. This holds for  $E_\vartheta$  and  $E_\phi$  as well as for the fields of the two dipoles, *viz*,  $\mathbf{E}^e$  and  $\mathbf{E}^m$ . Hence the position of point  $C$  between  $A$  and  $B$  is determined by the strength of the two dipole moments.

Indeed, the strength of the two dipole moments and by extension the proportionality between them are assessed by means of the ratio between  $E_\vartheta$  and  $E_\phi$ .

## 4.2. Validation

Let us now synthesize the approach described here above in light of the considerations elaborated in Section 3 for an antenna with unspecified geometry as illustrated in Fig. 3.

The procedure in the following is to demonstrate as rigorously as possible the existence of the LLP and the point of circular polarisation defined here above and then prove it by a simple example.

### 4.2.1. Lines of Linear Polarisation

The configuration of the electric and magnetic dipoles for an antenna of arbitrary geometry are displayed in Fig. 4. For this case, (8) are valid for the magnetic dipole and (10) describes the electric field produced by the electric dipole. LLP is given if

$$\mathbf{E}^e \times \mathbf{E}^m = \frac{E_e \cdot E_m}{r^2} (\sin \vartheta \cos \alpha - \sin \varphi \cos \vartheta \sin \alpha) \sin \vartheta \cdot \mathbf{e}_r = \mathbf{0}. \quad (14)$$

Equation (14) is fulfilled if

$$\sin \vartheta = 0 \quad (15a)$$

or

$$\sin \vartheta \cos \alpha - \sin \varphi \cos \vartheta \sin \alpha = 0. \quad (15b)$$

Solving (15a) after  $\vartheta$  yields

$$\sin \vartheta = 0 \Rightarrow \vartheta = n\pi; \quad n = 0, 1, 2, \dots \quad (16)$$

Equation (16) suggests that the LLP will pass through the point  $\vartheta = 0$  and/or its antipode  $\vartheta = \pi$ . Whether the LLP consists only of one curve passing simultaneously through the two points or two curves antipodal to one another each passing through one of the two points, depends to a large extent on the configuration of the antenna. The configuration of the dipoles chosen in this work allows us however to expect that the LLP above and below the equator are antipodal to one another as demonstrated here below.

Equation (15b) can be transformed into

$$\sin \varphi = \frac{\sin \vartheta}{\cos \vartheta} \cdot \frac{\cos \alpha}{\sin \alpha} = \tan \vartheta \cdot \cot \alpha. \tag{17}$$

It follows from (17) that the form of the LLP does not depend on the ratio between the amplitudes of the two elementary dipoles, but rather on the angle between their axes. These axes break through the sphere at points which lie along the LLP. At these points, the strength of the dipoles can be directly deduced.

Multiplying Equation (17) by  $r \cdot \sin \vartheta$  yields

$$r \cdot \sin \vartheta \sin \varphi = r \frac{\sin^2 \vartheta}{\cos \vartheta} \cot \alpha = r \frac{1 - \cos^2 \vartheta}{\cos \vartheta} \cot \alpha. \tag{18}$$

Transforming (18) by applying the relation  $\cos \vartheta = \frac{z}{r}$  and recognizing that  $y = r \sin \vartheta \sin \varphi$ , one obtains

$$y = \frac{r^2 - z^2}{z} \cot \alpha, \tag{19}$$

which may be rewritten in a more elaborated form as

$$z^2 + yz \cdot \tan \alpha = r^2. \tag{20}$$

Remembering now that  $r^2 = x^2 + y^2 + z^2$ , (20) turns to become

$$\begin{aligned} x^2 + y^2 - y \cdot z \tan \alpha &= 0 \\ \iff x^2 + \left(y - \frac{z}{2} \tan \alpha\right)^2 &= r_0^2, \end{aligned} \tag{21}$$

where  $r_0 = \frac{z}{2} \tan \alpha$ .

It is helpful to emphasize the geometric consequences of (21) for the structure of the LLP on the sphere. (21) is a non-linear equation, i.e., it does not represent a straight line. More precisely, it is a second-degree equation describing circles of varying radius that are all tangent at the point  $O(0,0)$  when mapped in the  $xy$ -plane, with  $z$  being an array parameter, also referred as the so-called schar-parameter (Fig. 6(c)). Hence the curve described by (17) does not lie in a plane. That means, on the surface of the sphere, the LLP is a closed second-order curve.

This curve can not pass simultaneously through the north pole in the upper hemisphere and through its antipodal point in the lower hemisphere. Otherwise, the LLP would become a circle around the sphere. As a consequence, the LLP would lie in a plane, in which case, the aforementioned result demonstrating that the LLP can not belong to a plane, is contradicted. Instead, we have two antipodal LLPs passing through the north pole for the first and through the south pole for the second and/or vice versa (Fig. 6(a)). That means,

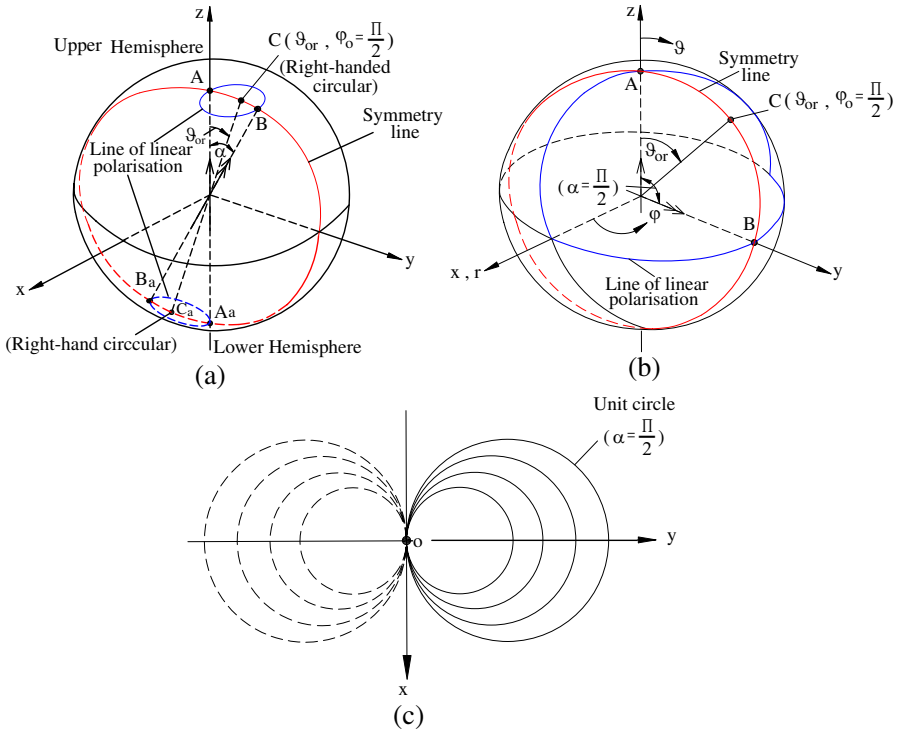


**Figure 6.** Sketches showing the line of linear polarisation, the symmetry line and the point of circular polarisation. (a) For an antenna of arbitrary geometry on the far field sphere and (b) for a patch antenna. The symmetry line is in general a circle but because of the ground, it is reduced to a semicircle in the case of the patch antenna. (c) Mapping of the line of linear polarisation in  $xy$ -plane as seen by an observer located on the upper hemisphere above the sphere (continuous lines), and on the lower hemisphere below the sphere (dotted lines).

given a point  $M$  on the LLP on the upper hemisphere of the far-field sphere with latitude  $\delta = \pi/2 - \vartheta$  and longitude  $\gamma$ , its antipode is a point  $M_a$  of latitude  $-\delta$  and longitude  $\gamma \pm \pi$  (the sign is taken so that the result is between  $-\pi$  and  $\pi$ ).

Recall that the north and south poles of the sphere are points where  $\vartheta = n\pi$ . Note also that the form of the curve on the sphere and the radius of the corresponding circle in the  $xy$ -plane are strongly dependent on the angle  $\alpha$  between the electric and magnetic dipole moments.

Two special cases are of particular interest: the case where the two dipole moments are parallel and the case where electric and magnetic

dipole are orthogonal.

If the two dipoles are parallel ( $\alpha = 0$ ), it is obvious that the LLP dwindles down to the north pole or its antipode counter part for the dipoles lying along the vertical  $z$  axis according to the chosen convention.  $A = B$ , and the wave is everywhere circular polarised.

For the special case of planar patch antennas as displayed in Fig. 4, the LLP is a curve lying along the equator ( $\alpha = \pi/2$ ) and the “Greenwich meridian” ( $\varphi = 0$  — Fig. 6(b)). The corresponding graph in the  $xy$ -plane is the unit circle (the largest one in Fig. 6(c)).

The preceding explanation is corroborated by simulation results on Fig. 7 displaying the phase angle difference  $m$

$$m = \phi_{E_\vartheta} - \phi_{E_\varphi} = \arctan \left( \frac{\Im(E_\vartheta)}{\Re(E_\vartheta)} \right) - \arctan \left( \frac{\Im(E_\varphi)}{\Re(E_\varphi)} \right), \quad (22)$$

between  $E_\vartheta$  and  $E_\varphi$  on the far field sphere for a dual-band PIFA (Fig. 8) at the resonant frequency  $f_1 = 990$  MHz and a resonant wire antenna of arbitrary geometry at  $f = 600$  MHz respectively. The bright blue curve (where  $m = 0$ ) in Fig. 7(a) and the yellow curve in Fig. 7(b) portray the LLP. As expected, the curves are closed lines.

Data displayed in Figs. 7 are gathered from simulation results in HFSS upon implementing Formula (22) in Matlab.

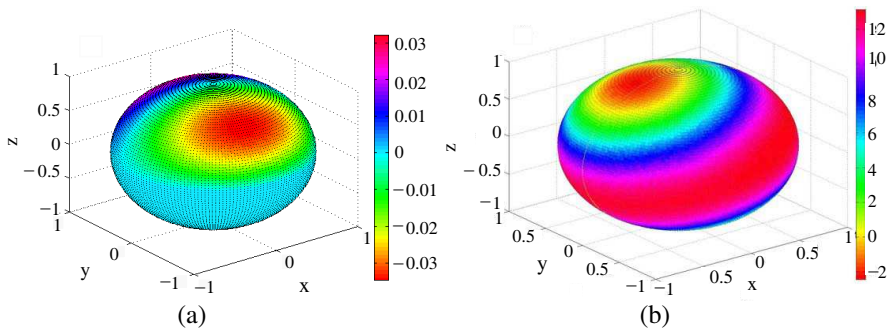


**Figure 7.** The function  $m$ . (a) For a PIFA at  $f_1 = 990$  MHz. Below the equator, all values are zero because of the ground plane of the antenna. The bright blue curve (where  $m = 0$ ) delineates the LLP. (b) For a wire antenna of arbitrary geometry resonant at  $f = 600$  MHz. The yellow curve ( $m = 0$ ) is the LLP. The antipodal character of  $m$  values is readily seen upon observation of the curves on the sphere. Note that  $m$  is just a consequence of the LLP analysis.

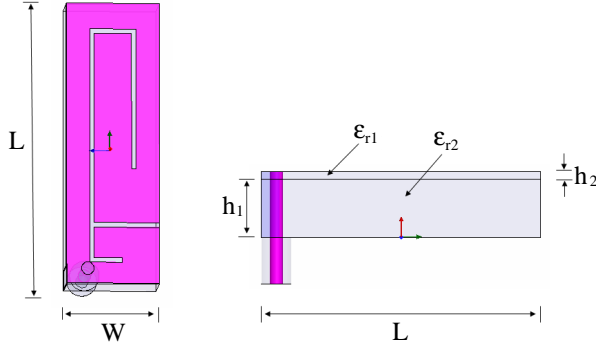


**Figure 8.** Simulated dual-band-PIFA. The antenna is of the same design as presented in [11]. PIFA stands for planar inverted antenna. Readers seeking for details about the antenna are kindly referred to the literature.

#### 4.2.2. Symmetry Line

In the phenomenology of the method, the symmetry line is defined as the line where the electric field components are orthogonal. Setting the scalar product of  $\mathbf{E}^e$  and  $\mathbf{E}^m$  equal to zero can help us to determine this line:

$$\mathbf{E}^e \cdot \mathbf{E}^m = \frac{E_e \cdot E_m}{r^2} \sin \vartheta \cos \varphi \sin \alpha \quad (23)$$

Equation (23) is equal to zero for

$$\sin \vartheta = 0 \implies \vartheta = n\pi; \quad n = 0, 1, 2, \dots \quad (24a)$$

or

$$\cos \varphi = 0 \implies \varphi = (2n + 1)\frac{\pi}{2}; \quad n = 0, 1, 2, \dots \quad (24b)$$

or

$$\sin \alpha = 0 \implies \alpha = n\pi; \quad n = 0, 1, 2, \dots \quad (24c)$$

In (24c),  $n$  only takes the value zero, since it is assumed throughout this work that  $0 \leq \alpha \leq \pi/2$ . For  $n = 0$ ,  $\alpha = 0$  and it follows that the two dipole moments are parallel. Moreover, the  $\vartheta$  component of the electric field of the magnetic dipole vanishes (Equation (8b)) and only its  $\varphi$  component remains. As a result,  $\mathbf{E}^e$  and  $\mathbf{E}^m$  are always orthogonal.

Let us now consider the case  $\alpha \neq 0$ . It follows from (24a) and (24b) that  $\mathbf{E}^e$  and  $\mathbf{E}^m$  are perpendicular to each other for  $\vartheta = n\pi$  or  $\varphi = (2n + 1)\frac{\pi}{2}$ .

In both cases, the symmetry line lies on the sphere surface. The line of equation  $\varphi = \pm\pi/2$  containing the points  $\vartheta = n\pi$  is for example a symmetry line. This is readily seen by verifying that  $E^m(\frac{\pi}{2} + \varphi) = E^m(\frac{\pi}{2} - \varphi)$  and  $E^e(\frac{\pi}{2} + \varphi) = E^e(\frac{\pi}{2} - \varphi)$ .

4.2.3. Line of Equal Amplitude and Point of Circular Polarisation

As you might have deduced from the section on the phenomenology of the approach, the point of circular polarisation is to be found along the symmetry line. Circular polarisation occurs when, in addition to the  $\pi/2$ -phase shift between  $\mathbf{E}_\vartheta = E_\vartheta \mathbf{e}_\vartheta$  and  $\mathbf{E}_\varphi = E_\varphi \mathbf{e}_\varphi$ , the two vectors are of equal amplitudes. It is therefore appropriate to put first more emphasis on the line of equal amplitudes before determining the point of circular polarisation.

a) *Line of equal amplitude:* Equal amplitudes,  $|E_\vartheta| = |E_\varphi|$ , are obtained, if the differential function  $p$  is equal to zero:

$$p = \sqrt{\Re(E_\vartheta)^2 + \Im(E_\vartheta)^2} - \sqrt{\Re(E_\varphi)^2 + \Im(E_\varphi)^2}. \tag{25}$$

Figure 9 displays the function  $p$ . From the legend of the graph, it is readily seen that the line of equal amplitudes is as predicted in the phenomenology of the approach, a closed line. It intersects the symmetry line at the point  $C$  which is the point of circular polarisation.

This point can also be rigorously determined mathematically as shown in the next subsection.

b) *The Point of Circular Polarisation:* Let us introduce the

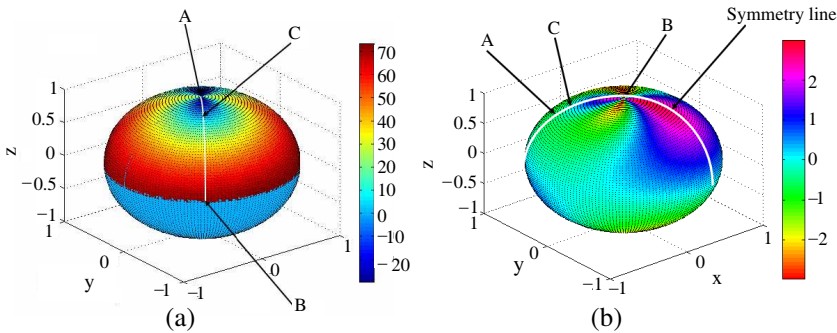


**Figure 9.** The function  $p$ . (a) For the dual-band-PIFA of Fig. 8 at resonant frequency  $f_1 = 900$  MHz. The white line indicates the symmetry line. (b) For a wire antenna of arbitrary geometry resonant at  $f = 600$  MHz.

modified polarisation ratio  $\eta$  as [3]

$$\eta = \pm jP, \quad (26)$$

where  $P$  is the polarisation ratio defined as quotient between  $E_{\vartheta}$  and  $E_{\varphi}$

$$P = \frac{E_{\vartheta}}{E_{\varphi}} = \frac{E_{\vartheta}^e + E_{\vartheta}^m}{E_{\varphi}^m} = \frac{E_m \cos \varphi \sin \alpha + E_e \sin \vartheta}{E_m (\sin \vartheta \cos \alpha - \sin \varphi \cos \vartheta \sin \alpha)}. \quad (27)$$

On the symmetry line ( $\varphi = \pi/2$ ) where the point of circular polarisation lies, the  $\vartheta$ -component of the magnetic dipole is zero.  $P$  is then reduced to

$$P = \frac{E_e \sin \vartheta}{E_m (\sin \vartheta \cos \alpha - \cos \vartheta \sin \alpha)} = \frac{E_e \sin \vartheta}{E_m \sin(\vartheta - \alpha)} = \frac{jE_e^0 \sin \vartheta}{E_m \sin(\vartheta - \alpha)}, \quad (28)$$

whence with  $\eta = jP$ , we get

$$\eta = \frac{-E_e^0 \sin \vartheta}{E_m \sin(\vartheta - \alpha)}. \quad (29)$$

Because of (10) and (11)  $P$  takes imaginary values, while  $\eta = \pm jP$  instead has real values. The point  $C$  can now be obtained by setting  $\eta = \pm 1$  for right and left circular polarisation respectively, since at  $C$  both components are of equal magnitude. We define  $C$  as point of coordinates  $(\varphi_0 = \pi/2, \vartheta_0)$ , where  $\vartheta_0$  is given by

$$\vartheta_{0r} = \arctan \left( \frac{E_m \sin \alpha}{E_e^0 + E_m \cos \alpha} \right) = \arctan \left( \frac{\sin \alpha}{\frac{E_e^0}{E_m} + \cos \alpha} \right), \quad (30a)$$

$$\vartheta_{0r} = \arctan \left( \frac{\sin \alpha}{1 + \cos \alpha} \right), \quad (30b)$$

for right circular polarisation and

$$\vartheta_{0i} = \arctan \left( \frac{E_m \sin \alpha}{E_m \cos \alpha - E_e^0} \right) = \arctan \left( \frac{\sin \alpha}{\cos \alpha - \frac{E_e^0}{E_m}} \right), \quad (31a)$$

$$\vartheta_{0i} = \arctan \left( \frac{\sin \alpha}{\cos \alpha - 1} \right), \quad (31b)$$

for left circular polarisation.

In (30) and (31), the subscripts  $r$  and  $l$  stand for right and left respectively.

From the foregoing investigation, two points of circular polarisation might exist. But do they both satisfy the topology? Are the two points within the domain of definition of  $\vartheta$ ? We are now going to prove the uniqueness of the point of circular polarisation.

The assumption placed earlier on the angle  $\alpha$  between the dipole moments suggests that  $\sin \alpha$  and  $\cos \alpha$  vary between 0 and 1. It follows that  $\cos \alpha - 1$  takes values between  $-1$  and  $0$  whereas  $1 + \cos \alpha$  belongs to the interval  $1$  to  $2$ . This leads respectively to negative arguments in (31b) and always positive values in (30b) for  $\alpha \neq 0$ . Hence  $\vartheta_{0_l}$  takes negative values which do not belong to the domain of definition of  $\vartheta$  while  $\vartheta_{0_r}$  always satisfies the topology. Consequently, only one point of circular polarisation exists, since the point of left circular polarisation does not satisfy the topology. This also holds for the boundary values of  $\alpha$ , i.e., for  $\alpha = 0$ , where  $\vartheta_{0_r} = 0^\circ$  and  $\vartheta_{0_l} = -90^\circ$ , and for  $\alpha = \pi/2$ , where  $\vartheta_{0_r} = 45^\circ$  and  $\vartheta_{0_l} = -45^\circ$ .

Recall that in spherical coordinates, the colatitude  $\vartheta$  runs from  $0$  to  $\pi$ .

$C$  is, together with the zeros of the electric dipole (point  $A$ ) and magnetic dipole (point  $B$ ) along the symmetry line, displayed on Figs. 6 and 9. It hardly needs to be pointed out that the zeros of the electric dipole on the symmetry line are given for  $\vartheta = n\pi$  and those of the magnetic dipole are obtained for  $\vartheta = (2n + 1)\pi/2$ ,  $n = 0, 1, 2, \dots$

Summing up, given simulated or measured data in the far field from an arbitrary electrically small antenna at resonance, the LLP:s are found upon displaying the phase difference  $m$  between  $E_\vartheta$  and  $E_\varphi$  on the far field sphere. These lines are closed curves of equation  $m = 0$  passing through the north pole or the south pole. The line where the electric field components are orthogonal is the symmetry line. Its shape is a circle lying on the sphere surface. This circle passes through the north and south poles and cuts the sphere into two equal parts. The line of equal amplitudes is, its side, determined by calculating the differential function  $p$  and portraying the obtained results on a sphere. The curve of equation  $p = 0$  is the sought-for-line. Its intersection with the symmetry line represents the point of circular polarisation.

## 5. POLARISATION STATES ON THE FAR-FIELD SPHERE

Having determined the peculiar loci in the field and validated the phenomenology of the approach, we would now proceed further and give a synoptic view of the different polarisation states described in the preceding sections on the far-field sphere. However, let's first provide a brief explanation on the difference and similarities between the far-field sphere and the well-known Poincaré sphere.

The Poincaré sphere is often used to visualize the state of polarisation of a plane wave [3, 10, 12, 13]. It has some similarities with the far-field sphere but should not be confused with the far-field sphere

used here. The Poincaré sphere is a sphere of radius  $S_0$ , whereby

$$S_0 = |E_x^2| + |E_y^2|$$

and of spherical angular coordinates  $2\tau$  and  $2\gamma$ , with

$$2\tau = \arctan\left(\frac{S_2}{S_1}\right) \quad \text{and} \quad 2\gamma = \sin\left(\frac{S_3}{S_0}\right)$$

being the latitude and longitude respectively [3, 12].  $S_1$ ,  $S_2$  and  $S_3$  are defined as

$$S_1 = |E_x^2| - |E_y^2|, \quad S_2 = 2|E_x||E_y| \cos \psi, \quad S_3 = 2|E_x||E_y| \sin \psi,$$

whereby  $|E_x|$ ,  $|E_y|$  are the component amplitudes of the wave and  $\psi$  is its phase difference.

The far-field sphere in turn, is a sphere with a geometrical radius  $r$ , with  $r$  being the distance from any point on the source to the observation point in far-field region.

On the surface of both spheres, Poincaré and far-field sphere, circular polarisations are visualized through single points. On the Poincaré sphere, north and south poles represent left-handed and right-handed circular polarisation respectively, while the equator is the LLP.

On contrary, on the far-field sphere, points of circular polarisation are not automatically located at the poles. Their location depends to a large extent on the configuration between the elementary electric dipole and the magnetic dipole moments. Moreover, the LLP is a closed curve on the surface of the sphere, whose form depends on the angle  $\alpha$  between the electric and magnetic dipole moments. This curve lies along the ‘‘Greenwich meridian’’ and the equator for  $\alpha = \pi/2$  (Figs. 6(b) and 10(b)). Elsewhere on the surface of the sphere, the polarisation is elliptical as on the Poincaré sphere.

The sense of polarisation on the far-field sphere can best be visualized along the symmetry line, since this line cuts not only the LLP, but also divides the sphere in two equal parts or semi-spheres. Fig. 11 shows the various states of polarisation. It is readily seen that we have four zones within which right-handed polarisation states (zones 1 and 3) alternate with left-handed states of polarisation (zone 2 and 4). The point of circular polarisation in the upper hemisphere is of the same state as its antipode in the lower hemisphere:  $C_a$  is antipodal to  $C$ . The same is valid for the LLPs: the LLP in the upper hemisphere is of identical state as its antipode in the lower hemisphere. These polarisation states can also be displayed as curves on the far-field sphere as depicted in Fig. 10(b).

We have discussed the polarization states with little mention of field polarization at the LLP and symmetry line intersection points  $A$  and  $B$ . Points  $A$ ,  $B$  are transition points of polarisation between the

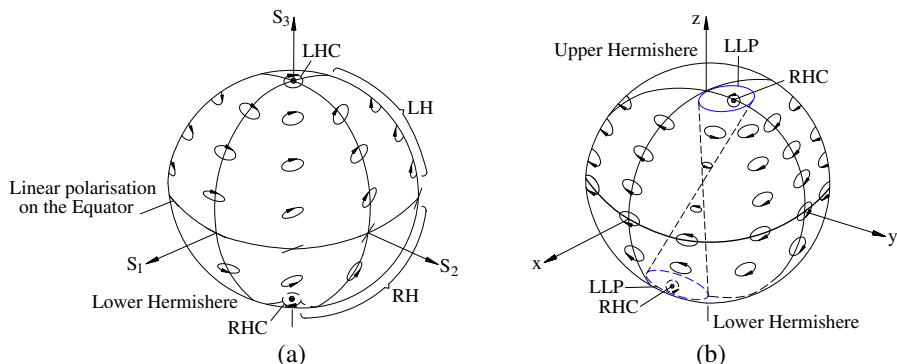


**Figure 10.** Representation of polarisation states. (a) On the Poincaré sphere. (b) On the far field sphere for  $0 < \alpha < 2/\pi$ . LH = Left-handed, LHC = Left-handed circular, RH = Right-handed, RHC = Right-handed circular and LLP = Line of linear polarisation.

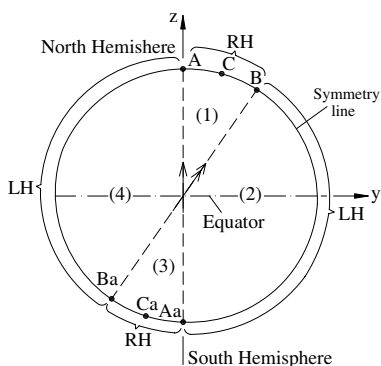


**Figure 11.** Visualization of polarisation senses along the symmetry line. RH means right-hand polarisation (zones 1 and 3) while LH stands for left-hand polarisation (zones 2 and 4).  $A_a$ ,  $B_a$  and  $C_a$  are antipodes of  $A$ ;  $B$ ; and  $C$ .  $C$  and  $C_a$  are points of circular polarisation.

right-hand (RH) and left-hand (LH) polarisations. Except for  $A = B$  (see discussion on the LLP in Subsection 2, Paragraph 1), the wave is at these points linear polarised, since the points belong to the LLP. The question is whether the polarisation is RH or LH.

Calculation of the limit values of the modified polarisation ratio, *eta*, left and right of  $A$  and  $B$  may help making a decision. The analytical procedure in this case is similar (but not totally identical!) to the discussion on the *Characterization of the Dipole Moments* in

the next section. It will therefore not be anticipated here. Rather, a graphical solution is presented for simplicity.

Observations of Fig. 11 show the following evidences: from the left of  $A$ , the field is LH-polarised whereas it is RH-polarised from the right. Further, from the left of  $B$ , the field is RH-polarised whereas it is LH-polarised from the right.

Similarly, we can analyze the antipodes  $A_a$  and  $B_a$ , which are themselves polarisation transition points. From the left (right) of  $A_a$ , the field is RH-polarised (LH-polarised). From the left of  $B_a$ , we see LH-polarisation while there is RH-polarisation from the right.

## 6. CHARACTERIZATION OF THE DIPOLE MOMENTS

In this section we will be dealing with the characterisation of the dipoles in dominant and non-dominant radiators. For identical reasons as for visualizing the sense of polarisation, this characterisation is carried out along the symmetry line. Moreover, the incoming investigations are carried out for LLP different from the symmetry line. For LLP and symmetry line coinciding, only one dipole exists. This case is left out here, as is not relevant for our discussion.

The ratio between the electric field component of the electric dipole and that of the magnetic dipole along the symmetry line is

$$\frac{E_{\vartheta}^e}{E_{\varphi}^m} = j \frac{E_e^0}{E_m} \cdot \frac{\sin \vartheta}{\sin(\vartheta - \alpha)} \quad (32)$$

At point  $C$ , the wave is right-handed circular polarised,  $\eta = 1$ , and we get from (29)

$$\frac{E_e^0}{E_m} = -\frac{\sin(\vartheta_{0r} - \alpha)}{\sin \vartheta_{0r}} \quad (33)$$

Replacing now the ratio  $\frac{E_e^0}{E_m}$  in (32) by its expression obtained in (33) yields

$$\frac{E_{\vartheta}^e}{E_{\varphi}^m} = -j \frac{\sin(\vartheta_{0r} - \alpha)}{\sin \vartheta_{0r}} \cdot \frac{\sin \vartheta}{\sin(\vartheta - \alpha)} = K \cdot \frac{\sin \vartheta}{\sin(\alpha - \vartheta)}, \quad (34)$$

where  $K = j \frac{\sin(\vartheta_{0r} - \alpha)}{\sin \vartheta_{0r}}$  is a constant. Equation (34) indicates that the ratio

$$\frac{\sin \vartheta}{\sin(\alpha - \vartheta)} \quad (35)$$

is a good figure of merit in characterizing which of the two dipoles is mainly responsible for radiation. Since simplicity usually leads

to clarity, we will first evaluate (35) graphically based on some few examples and then generalize obtained results. Note that in each of the forthcoming examples,  $\vartheta$  runs from 0 to  $\pi$ .

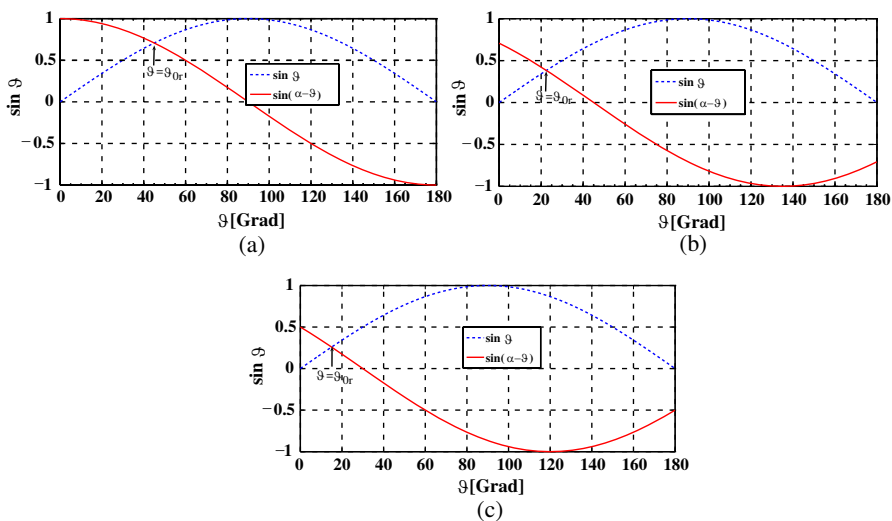
### 6.1. The Angle $\alpha$ Between the Dipoles is $\alpha = \frac{\pi}{2}$

Figure 12(a) displays the curves drawn by  $\sin(\alpha - \vartheta)$  and  $\sin \vartheta$ . It is readily seen that for:

- $0 \leq \vartheta < \frac{\pi}{4}$ ,  $\sin(\alpha - \vartheta) > \sin \vartheta$ , which means that the ratio  $\frac{\sin \vartheta}{\sin(\alpha - \vartheta)} < 1$ . As a result, the magnetic dipole dominates.
- $\vartheta > \frac{\pi}{4}$ ,  $\sin(\alpha - \vartheta) < \sin \vartheta$ . It follows that  $\frac{\sin \vartheta}{\sin(\alpha - \vartheta)} > 1$ ; the electric dipole is dominant.
- $\vartheta = \pi/4$ ,  $\sin(\alpha - \vartheta) = \sin \vartheta$ . This point corresponds to the point of circular polarisation  $C$ . The two dipoles are of equal magnitude.

### 6.2. $\alpha = \frac{\pi}{4}$ and $\alpha = \pi/6$

A synoptic view of Figs. 12(b) and 12(c) shows similar relationships between electric and magnetic dipoles as for  $\alpha = \pi/2$ . The point where  $\sin(\alpha - \vartheta) = \sin \vartheta$ , for both cases is the point of circular polarisation, since at this point  $\vartheta = \vartheta_{0,r}$  as can be verified upon calculating  $\vartheta_{0,r}$ .



**Figure 12.** The function  $\sin(\alpha - \vartheta)$  and  $(\sin \vartheta)$ . (a)  $\alpha = \frac{\pi}{2}$ . (b)  $\alpha = \frac{\pi}{4}$  and (c)  $\alpha = \frac{\pi}{6}$ .

from (30b). For  $\vartheta < \vartheta_{0,r}$  the radiation arises principally from the magnetic dipole and for  $\vartheta > \vartheta_{0,r}$  the radiation is predominantly electric.

Before generalizing insights already gained in this section it is worth noting that the examples discussed above substantiate the main result obtained in our discussion on the point of circular polarisation: the uniqueness of the point of circular polarisation on the far field sphere.

The foregoing investigations, together with the insight that at  $A$  the electric dipole has zero radiation and, at  $B$  no radiation of the magnetic dipole exists, allow us to draw the following general summary:

- For  $0 \leq \vartheta < \vartheta_{0,r}$ , i.e., between  $A$  and  $C$ , the radiation is predominantly magnetic.
- For  $\vartheta > \vartheta_{0,r}$ , the radiation is predominantly electric.

The characterization scheme above is a good figure of merit for an antenna engineer in deciding the antenna design: whether an antenna with a dominant electric dipole or an antenna showing a behavior of a magnetic dipole. This may be useful in mobile communication to avoid possible adverse effects of RF field on human health.

## 7. CONCLUSION

The radiation of electrically small resonant antennas has been decomposed into radiation from electric and magnetic dipoles upon applying successively the approach of assigning current density to dipole moments and the far field polarisation method. This approach provides a new valuable method for visualizing the state of polarisation on the far-field sphere with circular and linear polarisation being the main focus of interest. The first polarisation state arises only at one point on the symmetry line which cuts the sphere into two equal parts. The later one is along a closed line, the form of which depends on the angle between the dipole moments.

It is shown that the far field polarisation does not only allow the decomposition of more complicated cases, but also permits an easy characterization of dipole moments in dominant and non-dominant dipoles, thus providing some foresight to the antenna engineer. This figure of merit may help the antenna designer in making up his mind about the nature of the antenna being designed. The approach may also find application in EMC upon permitting the identification and characterisation of radiation sources of equipments under test. As a case of fact, in a PCB with an integrated antenna of known polarisation, this method may help in determining the presence of other radiation sources than the integrated antenna.

*Example:* Let us consider an antenna of arbitrary geometry integrated in a PCB and let's also suppose that the polarization of the antenna is known. Our task is to identify different radiation sources (if any) on the PCB.

The presented method may help us to determine the presence of radiation sources on the PCB other than that of the integrated antenna by comparing the polarization of the overall radiated field to that of the antenna. Should there be any difference, then other radiation sources do exist on the board.

An additional domain of application of the method might be the studies of scattering by electrically small objects.

### APPENDIX A. DERIVATION OF EQUATION (5) AND ITS TRANSFORMATION IN SPHERICAL COORDINATES

The cartesian coordinates  $x, y, z$  and  $x', y', z'$  may be transformed in spherical coordinate system as [10]

$$x = r \sin \vartheta \cos \varphi \tag{A1a}$$

$$y = r \sin \vartheta \sin \varphi \tag{A1b}$$

$$z = r \cos \vartheta \tag{A1c}$$

and

$$x' = r' \sin \vartheta' \cos \varphi' \tag{A2a}$$

$$y' = r' \sin \vartheta' \sin \varphi' \tag{A2b}$$

$$z' = r' \cos \vartheta' \tag{A2c}$$

respectively, and are related to each other by means of Equation (A3)

$$\begin{pmatrix} x' \\ y' \\ z' \end{pmatrix} = \underbrace{\begin{pmatrix} 1 & 0 & 0 \\ 0 & -\cos \alpha & \sin \alpha \\ 0 & -\sin \alpha & -\cos \alpha \end{pmatrix}}_M \cdot \begin{pmatrix} x \\ y \\ z \end{pmatrix} \tag{A3}$$

with  $M$  being the transformation matrix.

Upon setting (A1a)–(A1c) and (A2a)–(A2c) in (A3) one obtains

$$\begin{pmatrix} \sin \vartheta' \cos \varphi' \\ \sin \vartheta' \sin \varphi' \\ \cos \vartheta' \end{pmatrix} = M \cdot \begin{pmatrix} \sin \vartheta \cos \varphi \\ \sin \vartheta \sin \varphi \\ \cos \vartheta \end{pmatrix}. \tag{A4}$$

Carrying out the necessary algebra yields

$$\sin \vartheta' \cos \varphi' = \sin \vartheta \cos \varphi \tag{A5a}$$

$$\sin \vartheta' \sin \varphi' = -\sin \vartheta \sin \varphi \cos \alpha + \cos \vartheta \sin \alpha \tag{A5b}$$

$$\cos \vartheta' = -\sin \vartheta \sin \varphi \sin \alpha - \cos \vartheta \cos \alpha \tag{A5c}$$

(A5a)–(A5c) are the relationships between  $\vartheta$ ,  $\varphi$  and  $\vartheta'$ ,  $\varphi'$ . In the prime spherical coordinates  $\vartheta'$ ,  $\varphi'$ ,  $r'$  the electric field of the magnetic dipole is

$$\mathbf{E}^m = E_{\varphi'}^m (\mathbf{e}'_{\varphi}) = -\frac{E_m}{r} \cdot \sin \vartheta' \mathbf{e}'_{\varphi}, \quad (\text{A6})$$

which transformed in the prime Cartesian system turns to become

$$\mathbf{E}^m = \frac{E_m}{r} \begin{pmatrix} \sin \vartheta' \sin \varphi' \\ -\sin \vartheta' \cos \varphi' \\ 0 \end{pmatrix}. \quad (\text{A7})$$

In obtaining (A7), we applied the transformation relation from spherical to cartesian coordinates and also replaced  $\mathbf{e}'_{\varphi}$  by the following:  $\mathbf{e}'_{\varphi} = -\sin \varphi' \mathbf{e}'_x + \cos \varphi' \mathbf{e}'_y$ .

Having expressed the electric field of the magnetic dipole in the prime Cartesian system, it can now be transformed in the non-prime Cartesian coordinates. We have

$$\mathbf{E}^m = M^{-1} \cdot \frac{E_m}{r} \begin{pmatrix} \sin \vartheta' \sin \varphi' \\ -\sin \vartheta' \cos \varphi' \\ 0 \end{pmatrix},$$

where

$$M^{-1} = \begin{pmatrix} 1 & 0 & 0 \\ 0 & -\cos \alpha & -\sin \alpha \\ 0 & \sin \alpha & -\cos \alpha \end{pmatrix}.$$

In a more explicit form

$$\mathbf{E}^m = \frac{E_m}{r} \begin{pmatrix} \sin(\vartheta') \sin(\varphi') \\ \cos \alpha \sin \vartheta' \cos \varphi' \\ -\sin \alpha \sin \vartheta' \cos \varphi' \end{pmatrix}. \quad (\text{A8})$$

Setting now (A5a)–(A5c) in (A8), we get

$$\mathbf{E}^m = \frac{E_m}{r} \begin{pmatrix} -\cos \alpha \sin \vartheta \sin \varphi + \sin \alpha \cos \vartheta \\ \cos \alpha \sin \vartheta \cos \varphi \\ -\sin \alpha \sin \vartheta \cos \varphi \end{pmatrix}. \quad (\text{A9})$$

Equation (A9) is the sought for expression for the electric field of the magnetic dipole in the non-prime Cartesian coordinates. Transforming this expression in the non-prime spherical coordinates is a trivial process which is readily done.

$$\mathbf{E}^m = \frac{E_m}{r} A \cdot \begin{pmatrix} -\cos \alpha \sin \vartheta \sin \varphi + \sin \alpha \cos \vartheta \\ \cos \alpha \sin \vartheta \cos \varphi \\ -\sin \alpha \sin \vartheta \cos \varphi \end{pmatrix} \quad (\text{A10})$$

$A$  is the transformation matrix from Cartesian to spherical coordinates [10]

$$A = \begin{pmatrix} \sin \vartheta \cos \varphi & \sin \vartheta \sin \varphi & \cos \vartheta \\ \cos \vartheta \cos \varphi & \cos \vartheta \sin \varphi & -\sin \vartheta \\ -\sin \varphi & \cos \varphi & 0 \end{pmatrix}.$$

Carrying out the elementary calculus leads to

$$E_r^m = 0 \quad (\text{A11a})$$

$$E_\vartheta^m = \frac{E_m}{r} \cos(\varphi) \sin(\alpha) \quad (\text{A11b})$$

$$E_\varphi^m = \frac{E_m}{r} [\sin(\vartheta) \cos(\alpha) - \sin(\varphi) \cos(\vartheta) \sin(\alpha)] \quad (\text{A11c})$$

Note that a simplified representation of vectors has been chosen here above.

## REFERENCES

1. Chen, K. M. and J. C. Lin, "Biological effects of electromagnetic fields," *Handbook of Electromagnetic Compatibility*, R. Perez, Academic Press, San Diego, New York, Boston, etc., 1995.
2. Pouh e, D., G. M onich, and J. A. Tsemo Kamga, "Decomposition of electrically small resonant antennas into their electric and magnetic part by far field polarisation analysis," *Proc. EuCAP*, 428–432, Berlin, March 23–27, 2009.
3. Mott, H., *Polarisation in Antennas and Radar*, J. Willey & Sons, New York, Chichester, etc., 1986.
4. Rahola, J. and J. Krogerus, "On the polarization state of mobile terminals," *Proc. 12th. ICAP*, Vol. 2, 695–698, Exeter, March 31–April 3, 2003.
5. Hansen, W. W., "A new type of expansion in radiation problems," *Phys. Rev.*, Vol. 47, 139–143, 1935.
6. Stratton, J. A., *Electromagnetic Theory*, Chapter 7, IEEE Press, J. Wiley & Sons, 2007.
7. Harrington, R. F., "On the gain and beamwidth of directional antennas," *IRE AP-6*, 219–225, July 1958.
8. Ludwig, A. C., "Near-field far-field transformations using spherical-wave expansions," *IEEE Transactions on Antennas and Propagation*, Vol. 19, No. 2, 214–220, March 1971.
9. Zinke, O. and H. Brunswig, *Lehrbuch der Hochfrequenztechnik*, Kap. 6, Band 1, Springer-Verlag, Berlin, 1990.

10. Balanis, C. A., *Antenna Theory Analysis and Design*, 776, J. Willey & Sons, New York, Chichter, etc., 1982.
11. Huynh, M. C., *Wideband Compact Antennas for Wireless Communication Applications*, Dissertation, Virginia Poly. Inst. and State University, November 2004.
12. Smith, G. S., *An Introduction to Classical Electromagnetic Radiation*, Cambridge University Press, 1997.
13. Stutzman, W. L., *Polarization in Electromagnetic Systems*, Artech House, Boston, London, 1993.